A Shared-Control Strategy for Intelligent Wheelchairs Using Face Orientation and Potential Fields

Elias J. R. Freitas
Federal Institute of Minas Gerais, IFMG
Graduate Program in Electrical Engineering
Universidade Federal de Minas Gerais, UFMG
Av. Antônio Carlos 6627, 31270-901
Belo Horizonte, MG, Brazil
elias.freitas@ifmg.edu.br

Christyan H. Ribeiro
Department of Electronic Engineering
Universidade Federal de Minas Gerais, UFMG
Av. Antônio Carlos 6627, 31270-901
Belo Horizonte, MG, Brazil
ribeirochristyan9@gmail.com

Luciano C. A. Pimenta
Department of Electronic Engineering
Universidade Federal de Minas Gerais, UFMG
Av. Antônio Carlos 6627, 31270-901
Belo Horizonte, MG, Brazil
luciano.pimenta@gmail.com

***Abstract*—The wheelchair is an essential tool for the social integration of people with disabilities. The standard user interface for conventional electric wheelchairs is a joystick. However, some individuals, particularly the elderly and those with severe physical impairments, may be unable to use it. This paper proposes an alternative user interface for controlling wheelchairs based on face orientation. This interface uses a webcam to detect head movements in real time. The proposed method estimates yaw, pitch, and roll angles by extracting facial features from the image. A shared-control strategy based on potential fields is incorporated to enhance safety and usability, allowing the system to adjust or override user inputs when a LiDAR sensor detects obstacles. Simulation results demonstrate the approach's feasibility and effectiveness.**

***Index Terms*—intelligent wheelchair; shared-control; face orientation; potential fields.**

I. INTRODUCTION

Since the 20th century, the wheelchair has been one of the most important technological innovations for the social inclusion of people with physical disabilities or who, due to age, can no longer perform all tasks [1]. According to the United Nations Regional Information Center for Western Europe - UNRIC, 16% of the world's population has some form of disability [2]. In Brazil, this figure is about 8,4%, according to IBGE [3].

This work was carried out with the support of the Instituto Federal de Educação, Ciência e Tecnologia de Minas Gerais – Campus Ibirité, the Coordination for the Improvement of Higher Education Personnel - Brazil (CAPES) through the Academic Excellence Program (PROEX) and Finance Code 001. This work was also supported in part by the project INCT (National Institute of Science and Technology) under the grant CNPq (Brazilian National Research Council) 465755/2014-3 and FAPESP (São Paulo Research Foundation) 2014/50851-0, CNPq (grant numbers 315695/2020-0, 407063/2021-8, and 309925/2023-1), and Fundação de Amparo à Pesquisa do Estado de Minas Gerais (FAPEMIG), under grant numbers APQ-03090-17 and APQ-00630-23.

Recently, the scientific community has been working on new solutions for the social inclusion of these people. To achieve this goal, this work proposes applying intelligent features to a conventional wheelchair, such as obstacle avoidance, position and speed control, and new user interfaces. These wheelchairs are called Intelligent Wheelchairs (IW) [4].

A problem for many people, especially some elderly and those with some severe physical disabilities, such as those with Amyotrophic Lateral Sclerosis (ALS), is the inability to use the joystick in the motorized wheelchair. The interface approaches can be categorized into: voice control, biological control, and vision control. The most common interface is voice control because it is low-cost and easy to implement, many libraries are available, and it uses only a microphone. It's sometimes used alone [5, 6] or as an aid to the navigation system [7].

Considering biological control, some works show a brain-computer interface using Steady State Visually Evoked Potentials (SSVEP) [8], another shows an interface using the Electro-oculogram signal (EOG) [9], and still others use the electrical signals from the muscles of the face [10] or tongue [11] or using an accelerometer connected in the user's hand [12].

This paper focuses on interfaces based on computer vision techniques combined with a shared-safe control approach. Two approaches are commonly used as an interface: the first recognizes the intention of the user's head movement and the second recognizes the movement of the user's hand [13]. The most common hardware used is a webcam, but other works use the Kinect [14] or a stereo camera [15].

Traditional implementations in intelligent wheelchairs

(IWs) often rely solely on the pixel displacement of detected and tracked facial features to control speed [16, 17, 18]. Various techniques have been employed for face detection and tracking, such as the Adaboost algorithm for face detection, CAMShift (Continuously Adaptive Mean-Shift) for tracking [16], and optical flow methods [19]. Some approaches combine these techniques with the Kalman filter to enhance detection accuracy [20]. Other related works estimate face orientation using 3D model-based methods [21, 22] or structure-from-motion techniques [23].

Estimating face orientation provides an intuitive and non-invasive way to capture the user's intended movement. However, it does not guarantee safe navigation, such as avoiding obstacles in the environment. Thus, this paper proposes a shared control strategy that combines user intention, extracted from an accurate face orientation, with a safe autonomous navigation assistance based on potential fields. The proposed method uses feature detection in the image to estimate the head movement's yaw, pitch, and roll angles. At the same time, obstacle avoidance is handled by a repulsive potential field generated from a real-time LiDAR (*Light Detection and Ranging*) sensor.

The rest of the paper is organized as follows. Section II presents the methods, and Section III shows the results. Finally, the conclusions and future work are discussed in Section IV.

II. METHODS

This section describes our approach to enabling a person to safely guide a wheelchair (or another vehicle) using head movements. Fig. 1 illustrates the block diagram of the proposed approach composed of five steps: (A) Setup; (B) Image pre-processing; (C) Features detection; (D) Estimation of the face orientation, and (E) Shared-control. These steps are explained in detail in the following subsections.

A. Setup

The setup step provides the camera calibration parameters, obtaining the intrinsic parameters of the camera: (i) the focal lengths in pixels along the x and y axes (f_x, f_y), (ii) the skew between the x and y axes s, and (iii) the coordinates of the principal point (c_x, c_y). We assume that the distance between the user and the camera (Z_{calib}) remains constant, and that the user's body orientation, horizontally or vertically in the wheelchair, is practically unchanged. In addition, the distance between the center and the tip of the user's nose (Z_n) is given *a priori*.

B. Image pre-processing

First, since the webcam provides a noisy image, a Gaussian filter with a 5x5 mask is applied to reduce the noise in the image. The result is a blurred image, but with less noise.

Second, the RGB image is converted to the HSV color space, and only the brightness component (Value) is used.

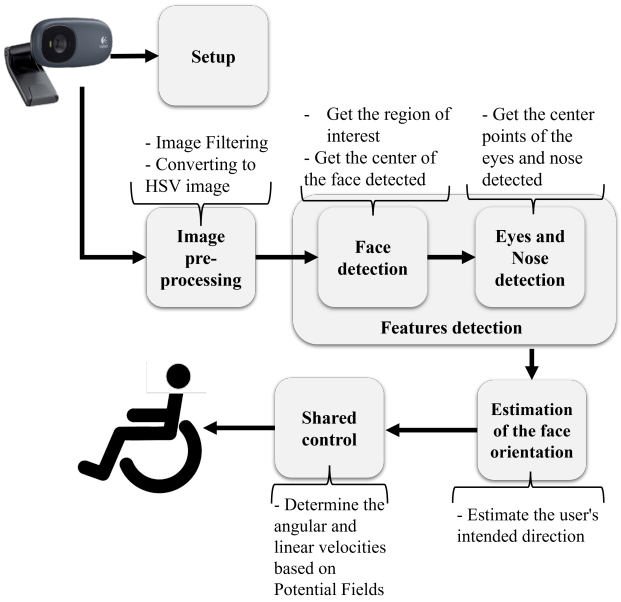

Fig. 1: Block diagram of the proposed approach.

The HSV color space separates color from intensity, which improves the detection of features in changing lighting conditions.

C. Features detection

Viola and Jones [24] proposed the Haar feature-based cascade classifiers, which allow high accuracy and speed for feature detection. The extracted features are based on features built from Haar wavelets, called the Haar-like features. This method consists of two stages. The first stage is the classifier's learning stage based on many positive and negative examples. The second stage is the detection stage, where this classifier is applied to the acquired images.

In this paper, we apply only the second stage, because for frontal face, eyes, and nose features, the classifier files corresponding to the first stage are available[1]. We have also used an open source Davis King's Dlib library [25] to get the center of the mouth, eyes, and nose tip. This Dlib provides 68 facial landmarks in a previously established landmark configuration. For that, it uses [26] a fast face alignment method using an ensemble of regression trees learned via gradient boosting.

D. Estimation of the face orientation

The estimation of the face orientation consists in the estimation of the angles: *pitch* (γ) corresponding to the orientation of the head to look up/down, *yaw* (β) corresponding to the orientation of the head to turn left/right and *roll* (α) corresponding to the orientation of the head to tilt left/right.

[1]https://github.com/Itseez/opencv/tree/master/data/haarcascades

In general, the related works [16], [17], and [18] use only approximate values or the rate of change of these angles (i.e., whether they are positive, zero, or negative), rather than the exact angle values. To estimate the angles more accurately, we propose the following geometric method.

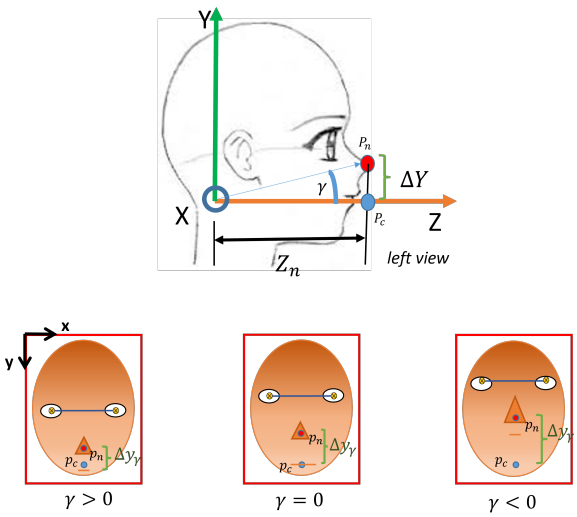

Fig. 2: The movement of the head to look up/down.

The movement of the head to look up/down, corresponding to the pitch angle (γ), is obtained based on Fig. 2 by:

$$\gamma = \arctan\left(\frac{\Delta y_\gamma \cdot Z_{calib}}{Z_n \cdot f_y}\right) - \gamma_0, \tag{1}$$

where Δy_γ is this difference observed in Fig. 2, p_n is the tip nose detected, p_c is the center of the mouth and γ_0 is the setup pitch angle, when the user is in the neutral front position.

The movement of the head turning to the left/right, corresponding to the yaw angle (β), is obtained similarly to the pitch angle, but now we look at the top view as shown in Fig. 3:

$$\beta = \arcsin\left(\frac{\Delta x_\beta \cdot Z_{calib}}{Z_n \cdot f_x}\right) - \beta_0, \tag{2}$$

where Δx_β is the difference observed in Fig. 3, and β_0 is the setup yaw angle when the user is in the neutral front position.

The tilting movement of the head, corresponding to the roll angle (α), can be obtained from the variation of the position $(\Delta x_\alpha, \Delta y_\alpha)$ of the detected eyes, as shown in Fig. 4:

$$\alpha = \arctan\left(\frac{\Delta y_\alpha \cdot f_y}{\Delta x_\alpha \cdot f_x}\right) - \alpha_0 \tag{3}$$

where α_0 is the setup yaw angle when the user is in the neutral front position.

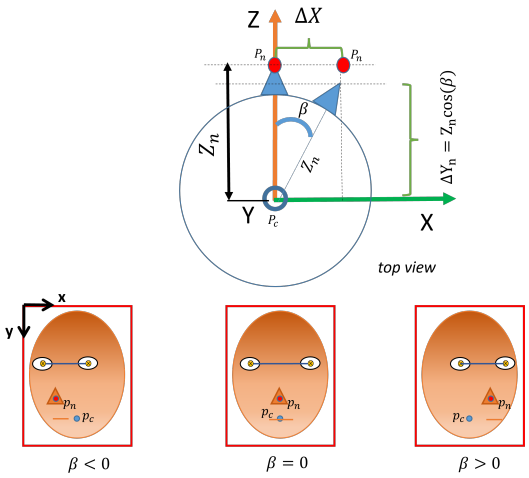

Fig. 3: The movement of the head turning to the left/right.

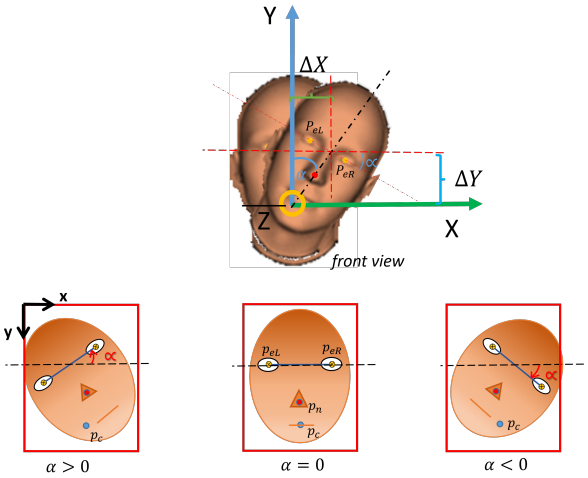

Fig. 4: The tilting movement of the head to left/right and the corresponding speed command.

E. Shared-control

The Artificial Potential Field is a reactive approach widely used in mobile robotics since the seminal work in [27]. The main idea of this approach is to model the robot's movement using virtual forces, where the goal target is considered an attractive potential pulling the robot towards it, and the obstacles are considered repulsive potentials that push the robot away. The total virtual force acting on the robot is given by the combination of these two components:

$$\mathbf{F}(\mathbf{q}) = \mathbf{F}_a(\mathbf{q}) + \mathbf{F}_r(\mathbf{q}), \tag{4}$$

where $\mathbf{q} = [x, y]^T$ is the robot's current position. $\mathbf{F}_a$ is defined according to the user's intention, estimated based on face orientation:

$$\mathbf{F}_a(\mathbf{q}) = k_a \cos(\gamma) \cdot \begin{bmatrix}\cos(\beta)\\ \sin(\beta)\end{bmatrix}, \tag{5}$$

where $k_a > 0$ is a scaling gain. In turn, the repulsive force is computed using LiDAR data, which provides N distance measurements between the robot and detected obstacles. Let $\mathbf{q}_{\text{obs}_i}$ denote the position of the i-th obstacle. Then, the repulsive force is:

$$\mathbf{F}_r(\mathbf{q}) = \sum_{i=1}^{N} \mathbf{F}_{r_i}, \tag{6}$$

where each component $\mathbf{F}_{r_i} = -\nabla U_{r_i}$ is derived from a repulsive potential field U_{r_i} defined as:

$$U_{\text{r}_i}(\mathbf{q}) = \begin{cases} \frac{1}{2} k_{\text{r}} \left(\frac{1}{\|\mathbf{q}_{obs_i} - \mathbf{q}\|} - \frac{1}{d_s} \right)^2 & \text{if } \|\mathbf{q}_{obs_i} - \mathbf{q}\| \leq d_s \\ 0 & \text{if } \|\mathbf{q}_{obs_i} - \mathbf{q}\| > d_s \end{cases}, \tag{7}$$

where $k_{\text{r}} > 0$ is a positive repulsive gain and d_s is the threshold distance beyond which the obstacle has no effect.

The wheelchair is modeled as a differential-drive robot, and the feedback linearization approach [28] is employed to map the resulting force vector into linear and angular velocity commands:

$$\begin{bmatrix} v \\ \omega \end{bmatrix} = \begin{bmatrix} \cos(\theta) & \sin(\theta) \\ -\frac{\sin(\theta)}{\ell} & \frac{\cos(\theta)}{\ell} \end{bmatrix} \cdot \mathbf{F}(\mathbf{q}), \tag{8}$$

where $l > 0$ is a virtual distance from the robot's center and θ represents the orientation of the wheelchair with respect to the global reference frame in the environment.

In addition, we defined a minimum pitch (γ) angle of 2^o to trigger forward acceleration of the wheelchair; otherwise, the wheelchair stays stopped.

III. RESULTS AND DISCUSSION

We implemented our proposed method in Python using the OpenCV library. The Robot Operating System (ROS)[29] was used as the middleware to manage communication between components. We employed the Turtlesim simulator (provided by the ROS framework) and the CoppeliaSim simulator [30] to simulate wheelchair motion. A built-in webcam was used for these experiments to capture the user's intention.

First, we used a GY-80 sensor, which is composed of a gyroscope, an accelerometer, and a magnetometer (an IMU, or inertial measurement unit), attached to the user's cap, to validate the obtained angles. Using the proposed method, we collected the measured IMU data and the angles for about three minutes. Fig. 6 shows this data for each angle. The maximum absolute error was less than ten degrees, and the average absolute error was less than five degrees.

The second experiment evaluates users' ability to issue head commands to follow a predefined rectangular path. For this experiment, we used the Turtlesim simulator. In this scenario, since the environment contains no obstacles, the reactive force component of the shared-control system is inactive. As shown in Fig. 7, the results indicate that

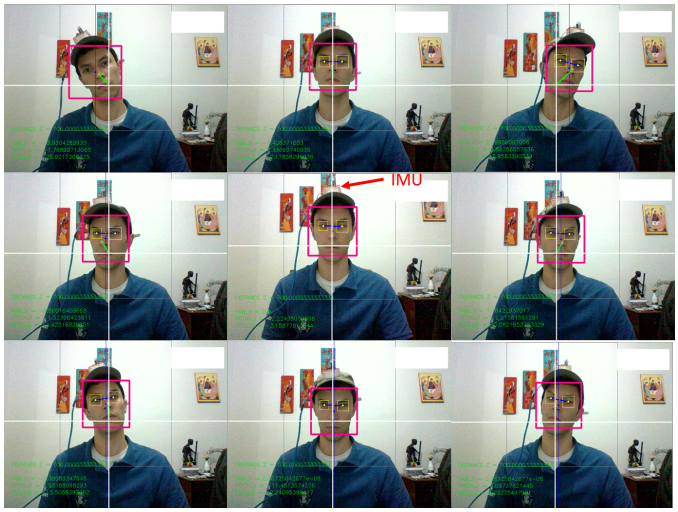

Fig. 5: Setup used to estimate angles for several face orientations.

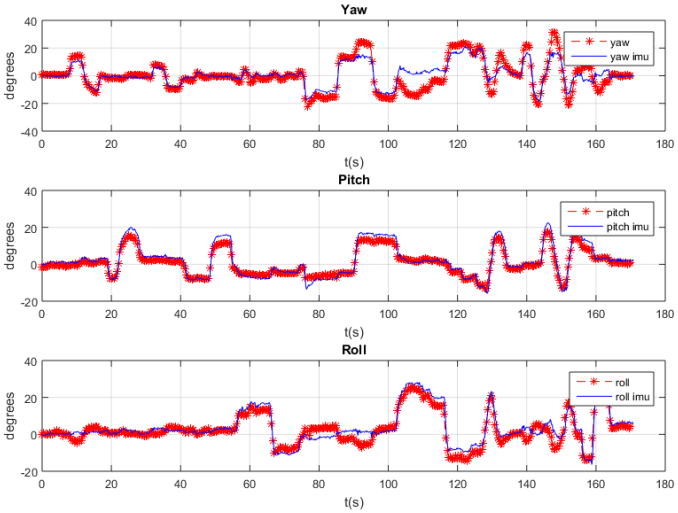

Fig. 6: Result of the measured IMU data and the angles obtained by the proposed method for each angle (yaw, pitch, and roll).

the user could roughly follow the desired trajectory. Additionally, this test highlights the importance of the shared-control strategy in an obstacle-filled environment, as precisely following a predefined path with head movements alone can also be challenging for the user, who may not be able to follow it precisely as intended.

The third experiment was conducted in the CoppeliaSim simulator using a wheelchair model with a Hokuyo LiDAR sensor. The test environment replicated a typical household layout to evaluate the system's performance. As in the previous experiment, the user attempted to follow a predefined path; however, obstacles were intentionally placed along the route. In this case, obstacle avoidance was handled by the proposed shared-control strategy, as illustrated in Fig. 8. A video demonstration of this exper-

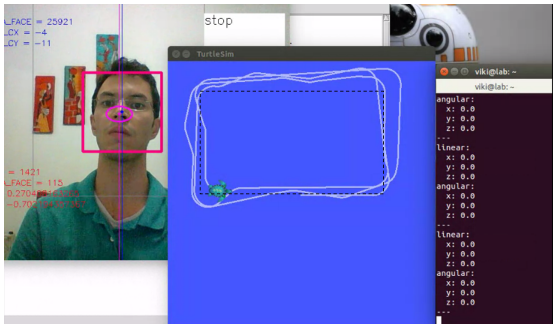

Fig. 7: Results for testing the head's commands to follow a predefined path without obstacles, using the Turtlesim simulator.

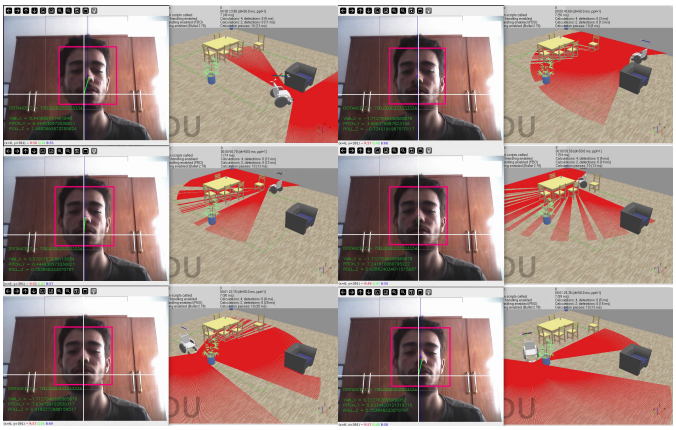

Fig. 8: Snapshots of the third experiment. More details in the video: https://youtu.be/xr0VEhpZTxU.

iment is available at: https://youtu.be/E45sTBP9lic.

Even when the user deliberately attempted to drive toward an obstacle, the system utilized LiDAR data to adjust the motion through the composition of potential fields, enabling safe navigation. Fig. 9 shows the complete path followed by the wheelchair.

IV. CONCLUSION

This paper proposed an approach for estimating the orientation angles of the user's face combined with a shared-control strategy for Intelligent wheelchairs. The results suggest that this methodology is promising for real-world applications, enabling users to move in any direction. We achieved low absolute errors in angle estimation. Furthermore, integrating a shared-control strategy based on potential fields significantly improves safety by helping users avoid collisions. Even when a user unintentionally attempts to move toward an obstacle, the system can adaptively adjust the motion to ensure safe and smooth navigation.

The potential field approach could be improved by adjusting the repulsive field's activation distance, potentially through a gain adjustment to the LiDAR input. The use of 2D LiDAR raises concerns about detecting

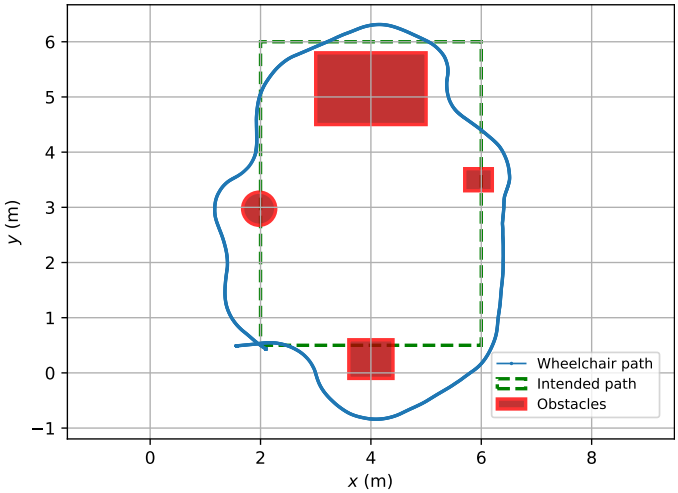

Fig. 9: The path followed by the wheelchair (in blue) for the experiment in Fig. 8. The user's intended path is shown in a green dashed line.

taller objects, such as table edges, which could compromise safety. Exploring 3D sensing could address this limitation.

In future work, we plan to implement the proposed strategy on a real wheelchair. We aim to enhance safety through improved speed control, particularly when facial features are not detected, unintended user movements occur, or local minima arise due to the potential field approach. To address the local minima problem, we may employ a more advanced strategy based on an anytime planner that uses only local information, as proposed in our previous work [31, 32]. Additionally, we intend to address current limitations such as the assumption of a fixed distance, constant orientation between the user's face and the camera, and a known nose position. To overcome these constraints, we will investigate using stereo cameras, among other alternatives.

References

[1] IHT, "A historical sociology of the wheelchair," Innovative Health Technologies, 2016. [Online]. Available: http://www.york.ac.uk/res/iht/projects/l218252007.htm

[2] U. N. R. I. C. for Western Europe, "Building an accessible future for all: Ai and the inclusion of persons with disabilities," 2024. [Online]. Available: https://tinyurl.com/kjsxzx4h

[3] I. Gomes, "Pessoas com deficiência têm menor acesso à educação, ao trabalho e à renda," 2023. [Online]. Available: https://tinyurl.com/4e3xd2yu

[4] B. M. Faria, L. P. Reis, and N. Lau, "A survey on intelligent wheelchair prototypes and simulators," in *Advances in Intelligent Systems and Computing*. Springer Science Business Media, 2014, pp. 545–557. [Online]. Available: http://dx.doi.org/10.1007/978-3-319-05951-8_52

[5] P. P. Dutta, A. Kumar, A. Singh, K. Saha, B. Hazarika, A. Narzary, and T. Sharma, "Design and development of voice controllable wheelchair," in *2020 8th International Conference on Reliability, Infocom Technologies and Optimization (Trends and Future Directions)(ICRITO)*. IEEE, 2020, pp. 1004–1008.

[6] K. Anam, A. Saleh *et al.*, "Voice controlled wheelchair for disabled patients based on cnn and lstm," in *2020 4th International Conference on Informatics and Computational Sciences (ICICoS)*. IEEE, 2020, pp. 1–5.

[7] S. Anwer, A. Waris, H. Sultan, S. I. Butt, M. H. Zafar, M. Sarwar, I. K. Niazi, M. Shafique, and A. N. Pujari, "Eye and voice-controlled human machine interface system for wheelchairs using image gradient approach," *Sensors*, vol. 20, no. 19, p. 5510, 2020.

[8] N. Siribunyaphat and Y. Punsawad, "Brain–computer interface based on steady-state visual evoked potential using quick-response code pattern for wheelchair control," *Sensors*, vol. 23, no. 4, p. 2069, 2023.

[9] A. Golrou, N. Rafiei, and M. Sabouri, "Wheelchair controlling by eye movements using eog based human machine interface and artificial neural network," *Int J Comput Appl*, vol. 975, p. 8887, 2022.

[10] M. K. Shahin, A. Tharwat, T. Gaber, and A. E. Hassanien, "A wheelchair control system using human-machine interaction: Single-modal and multimodal approaches," *Journal of Intelligent Systems*, vol. 28, no. 1, pp. 115–132, 2019.

[11] E. R. Lontis, B. Bentsen, M. Gaihede, F. Biering-Sørensen, and L. N. A. Struijk, "Wheelchair control with inductive intra-oral tongue interface for individuals with tetraplegia," *IEEE Sensors Journal*, vol. 21, no. 20, pp. 22 878–22 890, 2021.

[12] I. Miftahussalam, E. S. Julian, K. Prawiroredjo, and E. Djuana, "Wheelchair control system with hand movement using accelerometer sensor," *Microelectronic Engineering*, vol. 278, p. 112018, 2023.

[13] M. Repon Islam, M. Saiful Islam, and M. S. Sadi, "Towards developing a real-time hand gesture controlled wheelchair," in *Proceedings of International Conference on Trends in Computational and Cognitive Engineering: Proceedings of TCCE 2020*. Springer, 2020, pp. 355–366.

[14] H. Hamadi, B. Suhendro, M. Alamsyah, and M. Ibrahim, "Human tracking control system using kinect sensors on wheelchair based on arduino," in *Journal of Physics: Conference Series*, vol. 1436, no. 1. IOP Publishing, 2020, p. 012003.

[15] E. Sola-Thomas, M. A. B. Sarker, M. V. Caracciolo, O. Casciotti, C. D. Lloyd, and M. H. Imtiaz, "Design of a low-cost, lightweight smart wheelchair," in *2021 IEEE Microelectronics Design & Test Symposium (MDTS)*. IEEE, 2021, pp. 1–7.

[16] P. Jia, H. H. Hu, T. Lu, and K. Yuan, "Head gesture recognition for hands-free control of an intelligent wheelchair," *Industrial Robot*, vol. 34, no. 1, pp. 60–68, jan 2007. [Online]. Available: http://dx.doi.org/10.1108/01439910710718469

[17] Y. Kuno, N. Shimada, and Y. Shirai, "A robotic wheelchair based on the integration of human and environmental observations - look where youŕe going," *IEEE Robotics Automation Magazine*, vol. 10, no. 1, pp. 26–34, mar 2003. [Online]. Available: http://dx.doi.org/10.1109/MRA.2003.1191708

[18] C. Noiruxsar and P. Samanpiboon, "Face Orientation Recognition for Electric Wheelchair Control," *Journal of Automation and Control Engineering*, vol. 2, no. 4, pp. 402–405, 2014.

[19] Y. Adachi, Y. Kuno, N. Shimada, and Y. Shirai, "Intelligent wheelchair using visual information on human faces," in *Proceedings. 1998 IEEE/RSJ International Conference on Intelligent Robots and Systems. Innovations in Theory, Practice and Applications (Cat. No.98CH36190)*. Institute of Electrical & Electronics Engineers (IEEE), 1998. [Online]. Available: http://dx.doi.org/10.1109/IROS.1998.724645

[20] W. Yu and L. Gang, "Head pose estimation based on head tracking and the kalman filter," *Physics Procedia*, vol. 22, pp. 420–427, 2011. [Online]. Available: http://dx.doi.org/10.1016/j.phpro.2011.11.066

[21] Y. Yari and J. Scharcanski, "An approach for fast human head pose estimation," in *Mobile Multimedia/Image Processing, Security, and Applications 2011*, S. S. Agaian, S. A. Jassim, and Y. Du, Eds. SPIE-Intl Soc Optical Eng, may 2011. [Online]. Available: http://dx.doi.org/10.1117/12.884138

[22] Y. Xu, J. Zeng, and Y. Sun, "Head pose recovery using 3d cross model," in *2012 4th International Conference on Intelligent Human-Machine Systems and Cybernetics*. Institute of Electrical Electronics Engineers (IEEE), aug 2012. [Online]. Available: http://dx.doi.org/10.1109/IHMSC.2012.111

[23] A. Pernek and L. Hajder, "Precise 3d pose estimation of human faces," in *Computer Vision Theory and Applications (VISAPP), 2014 International Conference on*, vol. 3, Jan 2014, pp. 618–625.

[24] P. Viola and M. Jones, "Rapid object detection using a boosted cascade of simple features," in *Proceedings of the 2001 IEEE Computer Society Conference on Computer Vision and Pattern Recognition. CVPR 2001.* Institute of Electrical & Electronics Engineers (IEEE), 2001. [Online]. Available: http://dx.doi.org/10.1109/CVPR.2001.990517

[25] D. E. King, "Dlib-ml: A machine learning toolkit," *Journal of Machine Learning Research*, vol. 10, pp. 1755–1758, 2009.

[26] V. Kazemi and J. Sullivan, "One millisecond face alignment with an ensemble of regression trees," in *Proceedings of the 2014 IEEE Conference on*

Computer Vision and Pattern Recognition, ser. CVPR '14. Washington, DC, USA: IEEE Computer Society, 2014, pp. 1867–1874. [Online]. Available: http://dx.doi.org/10.1109/CVPR.2014.241

[27] O. Khatib, "Real-time obstacle avoidance for manipulators and mobile robots," *The international journal of robotics research*, vol. 5, no. 1, pp. 90–98, 1986.

[28] M. W. Spong, S. Hutchinson, M. Vidyasagar *et al.*, *Robot modeling and control*. Wiley New York, 2006, vol. 3.

[29] M. Quigley, B. Gerkey, K. Conley, J. Faust, T. Foote, J. Leibs, R. Wheeler, and A. Y. Ng, "Ros: an open-source robot operating system," in *ICRA Workshop on Open Source Software*, vol. 3, no. 3.2, 2009, p. 5.

[30] C. R. GmbH, "Coppeliasim: Robot simulator," https://www.coppeliarobotics.com/, 2024, accessed: 2025-05-28.

[31] G. A. Pereira and E. J. Freitas, "Navigation of semi-autonomous service robots using local information and anytime motion planners," *Robotica*, vol. 38, no. 11, pp. 2080–2098, 2020.

[32] E. J. Freitas, H. Passos, and G. A. Pereira, "Desvio de obstáculos por robôs semiautônomos usando planejamento de caminhos," *XIII Simpósio Brasileiro de Automação Inteligente*, pp. 1043–1048, 2017.